University of Nebraska - Lincoln
DigitalCommons@University of Nebraska - Lincoln

Biochemistry -- Faculty Publications | Biochemistry, Department of

2011

RpiR Homologues May Link *Staphylococcus aureus* RNAIII Synthesis and Pentose Phosphate Pathway Regulation

Yefei Zhu
University of Nebraska-Lincoln

Nandakumar Madayiputhiya
University of Nebraska - Lincoln, nmadayiputhiya2@unl.edu

Marat R. Sadykov
University of Nebraska-Lincoln

Nandakumar Madayiputhiya
University of Nebraska - Lincoln

Thanh T. Luong
University of Arkansas for Medical Sciences

See next page for additional authors

Authors
Yefei Zhu, Nandakumar Madayiputhiya, Marat R. Sadykov, Nandakumar Madayiputhiya, Thanh T. Luong, Rosmarie Gaupp, Chia Y. Lee, and Greg Somerville

Journal of Bacteriology, Nov. 2011, p. 6187–6196 Vol. 193, No. 22
0021-9193/11/$12.00 doi:10.1128/JB.05930-11

RpiR Homologues May Link *Staphylococcus aureus* RNAIII Synthesis and Pentose Phosphate Pathway Regulation▽†

Yefei Zhu,[1] Renu Nandakumar,[2] Marat R. Sadykov,[1] Nandakumar Madayiputhiya,[2] Thanh T. Luong,[3] Rosmarie Gaupp,[1] Chia Y. Lee,[3] and Greg A. Somerville[1]*

School of Veterinary Medicine and Biomedical Sciences, University of Nebraska—Lincoln, Lincoln, Nebraska 68583–0905[1]; Proteomics and Metabolomics Core, Redox Biology Center, Department of Biochemistry, University of Nebraska, Lincoln, Nebraska 68588[2]; and Department of Microbiology and Immunology, University of Arkansas for Medical Sciences, Little Rock, Arkansas[3]

Received 3 August 2011/Accepted 7 September 2011

***Staphylococcus aureus* is a medically important pathogen that synthesizes a wide range of virulence determinants. The synthesis of many staphylococcal virulence determinants is regulated in part by stress-induced changes in the activity of the tricarboxylic acid (TCA) cycle. One metabolic change associated with TCA cycle stress is an increased concentration of ribose, leading us to hypothesize that a pentose phosphate pathway (PPP)-responsive regulator mediates some of the TCA cycle-dependent regulatory effects. Using bioinformatics, we identified three potential ribose-responsive regulators that belong to the RpiR family of transcriptional regulators. To determine whether these RpiR homologues affect PPP activity and virulence determinant synthesis, the *rpiR* homologues were inactivated, and the effects on PPP activity and virulence factor synthesis were assessed. Two of the three homologues (RpiRB and RpiRC) positively influence the transcription of the PPP genes *rpiA* and *zwf*, while the third homologue (RpiRA) is slightly antagonistic to the other homologues. In addition, inactivation of RpiRC altered the temporal transcription of RNAIII, the effector molecule of the *agr* quorum-sensing system. These data confirm the close linkage of central metabolism and virulence determinant synthesis, and they establish a metabolic override for quorum-sensing-dependent regulation of RNAIII transcription.**

Staphylococcus aureus is an important human and animal pathogen that is capable of infecting nearly all host anatomic sites. The pathogenicity of *S. aureus* depends on its ability to synthesize virulence factors that facilitate colonization, immune evasion, and nutrient acquisition. Virulence factor synthesis is controlled by a complex network of regulatory proteins, including the *agr* quorum-sensing system and the SarA family of regulators (6, 29). In addition, tricarboxylic acid (TCA) cycle activity is important for the regulation of staphylococcal virulence factor synthesis (33, 39–41, 48). Since the two most common types of regulation are genetic regulation and metabolic regulation, TCA cycle-dependent regulation most likely occurs via one or both of these mechanisms. Genetic regulation occurs through the repression or induction of enzyme synthesis, while metabolic regulation controls enzyme activity through the availability of substrates and cofactors. An example of staphylococcal metabolic regulation is the synthesis of capsular polysaccharide, which is regulated by TCA cycle activity through the supply of phosphoenolpyruvate for gluconeogenesis (33). Other virulence factors, such as polysaccharide intercellular adhesin (PIA), are genetically regulated by TCA cycle activity through transcriptional repression of the operon encoding the enzymes of PIA biosynthesis (i.e., *icaADBC*) (34, 44). This TCA cycle-dependent genetic regulation likely depends on response regulators that react to metabolic changes associated with TCA cycle activity fluctuations (35, 41).

In *Staphylococcus epidermidis*, TCA cycle stress (i.e., any environmental stressor, such as iron limitation, that is capable of altering TCA cycle activity) increases the intracellular ribose concentration, indicating that carbon flow through the pentose phosphate pathway (PPP) is increased during TCA cycle stress (35). This suggests that if there is a regulator that can respond to the concentration of ribose, or another PPP metabolite, then the activity of that regulator will likely be altered. The PPP-responsive regulator prototype, RpiR, was first identified in *Escherichia coli* as a regulator of ribose-5-phosphate isomerase B (*rpiB*), which catalyzes the reversible isomerization of ribulose-5-phosphate and ribose-5-phosphate (42). Members of the RpiR family often act as transcriptional regulators of sugar catabolism, and RpiR homologues have been identified as repressors and activators in both Gram-negative and Gram-positive bacteria, including *E. coli*, *Pseudomonas putida*, and *Bacillus subtilis* (8, 42, 46). As sugar-responsive regulators, members of the RpiR family of proteins have N-terminal helix-turn-helix DNA binding motifs and C-terminal sugar isomerase binding (SIS) domains (1).

TCA cycle stress alters the intracellular ribose concentration in *S. epidermidis* and also alters the temporal expression of virulence factors in *S. epidermidis* and *S. aureus* (34, 35, 39, 40). These observations led us to hypothesize that an RpiR homologue may link the PPP to virulence factor regulation in staph-

* Corresponding author. Mailing address: School of Veterinary Medicine and Biomedical Sciences, University of Nebraska—Lincoln, 155 VBS, Fair St. and East Campus Loop, Lincoln, NE 68583-0905. Phone: (402) 472-6063. Fax: (402) 472-9690. E-mail: gsomerville3@unl.edu.

† Supplemental material for this article may be found at http://jb.asm.org/.

▽ Published ahead of print on 16 September 2011.

TABLE 1. Strains and plasmids used in this study

Plasmid or strain	Relevant genotype and/or characteristic(s)[a]	Source or reference
Plasmids		
pBluescript II KS(+)	*E. coli* phagemid cloning vector	Stratagene
pTS1	*S. aureus-E. coli* temperature-sensitive shuttle vector; Amp^r Cam^r	14
pTS1-d	Derivative of pTS1 with deletion of plasmid-encoded 3′ region of *ermC*	34
pEC4	pBluescript II KS(+) with *ermB* inserted into ClaI site	3
pJF12	Plasmid pCR2.1 containing *tetM*; Amp^r Min^r	J. Finan and G. Archer
pYF-7	pBluescript II KS(+) containing a portion of SAV0317	This study
pYF-8	pYF-7 containing an *ermB* cassette inserted into the NdeI site of SAV0317	This study
pYF-9	SAV0317::*ermB* product from pYF-8 inserted into BamHI/SacI-digested pTS1	This study
pYM-4	Derivative of pTS1 with SAV0193::*cat* fragment	This study
pYM-5	Derivative of pTS1 with SAV2315::*tetM* fragment	This study
pCL15	Expression vector; derivative of pSI-1; Cam^r	Chia Lee
pCL15-*ermB*	Replacement of *cat* with *ermB* in expression plasmid pCL15; Erm^r	This study
pYF-10	pCL15 with the SAV0317 gene under the control of the P_{spac} promoter; Cam^r	This study
pYF-11	pCL15-*ermB* with the SAV0193 gene under the control of the P_{spac} promoter; Erm^r	This study
pYF-12	pCL15 with the SAV2315 gene under the control of the P_{spac} promoter; Cam^r	This study
Strains		
RN4220	Restriction-negative *S. aureus*	30
DH5α	*E. coli* cloning host	Invitrogen
UAMS-1	*S. aureus* clinical isolate	13
UAMS-1-*rpiRA*	SAV0317 insertion mutant of UAMS-1; Erm^r	This study
UAMS-1-*rpiRB*	SAV0193 deletion mutant of UAMS-1; Cam^r	This study
UAMS-1-*rpiRC*	SAV2315 deletion mutant of UAMS-1; Min^r	This study
UAMS-1-*rpiRAB*	SAV0317 SAV0193 double mutant of UAMS-1; Erm^r Cam^r	This study
UAMS-1-*rpiRAC*	SAV0317 SAV2315 double mutant of UAMS-1; Erm^r Min^r	This study
UAMS-1-*rpiRBC*	SAV0193 SAV2315 double mutant of UAMS-1; Cam^r Min^r	This study
UAMS-1-*rpiRABC*	SAV0317 SAV0193 SAV2315 triple mutant of UAMS-1; Erm^r Cam^r Min^r	This study

[a] Amp^r, ampicillin resistant; Cam^r, chloramphenicol resistant; Erm^r, erythromycin resistant; Min^r, minocycline resistant.

ylococci. A search of the *S. aureus* strain Mu50 genome (18) returned three open reading frames (ORFs) with significant amino acid homology to RpiR (21 to 23% amino acid identity and 45 to 46% amino acid similarity): SAV0317, SAV0193, and SAV2315. For simplicity, these homologues were designated RpiRA (SAV0317), RpiRB (SAV0193), and RpiRC (SAV2315). To determine whether these RpiR homologues link the PPP to virulence factor synthesis in *S. aureus*, three single mutants, three double mutants, and a triple mutant of the *rpiR* homologues were constructed in *S. aureus* strain UAMS-1, and the effects on PPP activity, RNAIII transcription, capsular polysaccharide biosynthesis, PIA accumulation, and the ability to form a biofilm were assessed.

MATERIALS AND METHODS

Bacterial strains and growth conditions. The strains and plasmids used in this study are listed in Table 1. *E. coli* strains were grown in 2× YT broth (36) or on 2× YT agar, and *S. aureus* strains were grown in tryptic soy broth (TSB) (BD Biosciences) or on TSB containing 1.5% agar. TSB is a complex medium that contains glucose (0.25%, wt/vol) and stachyose. Stachyose is a plant carbohydrate that *S. aureus* cannot catabolize. Unless otherwise stated, all bacterial cultures were inoculated at 1:200 from an overnight culture (normalized for growth) into TSB, incubated at 37°C, and aerated at 225 rpm with a flask-to-medium ratio of 10:1. Antibiotics were purchased from Fisher Scientific or Sigma Chemical and, when used, were used at the following concentrations: for *E. coli*, ampicillin at 100 μg/ml; for *S. aureus*, erythromycin at 8 or 10 μg/ml, chloramphenicol at 10 to 15 μg/ml, and tetracycline at 10 μg/ml.

Construction of *S. aureus rpiR* mutants. To inactivate *rpiRA* (ORF SAV0317), a 2.559-kb fragment was PCR amplified using primers SAV0316-BamHI and SAV0318-SacI (Table 2), and the product was cloned into the SmaI site of pBluescript II KS(+) (Stratagene) to generate plasmid pYF-7. The *ermB* cassette of pEC4 was amplified using primers pEC4ErmBNdeIF and pEC4ErmBNdeIR (Table 2) and was ligated into the NdeI site within *rpiRA* of pYF-7 to yield plasmid pYF-8. The *rpiRA*::*ermB* fragment of pYF-8 was cloned into the BamHI and SacI sites of pTS1 to create plasmid pYF-9. The temperature-sensitive plasmid pYF-9 was isolated from *S. aureus* strain RN4220 and was introduced into strain UAMS-1 by electroporation. Transformed bacteria were used to construct the *rpiRA* mutant using the temperature shift method of Foster (11).

To inactivate *rpiRB* (ORF SAV0193), the technique of gene splicing by overlap extension (15) was used to replace a 741-bp internal region of *rpiRB* with the *cat* gene from plasmid pTS1. For PCR, genomic DNA from *S. aureus* strain UAMS-1 was used as a template for the amplification of regions flanking *rpiRB*. PCR primers BamHI-SAV0192-f and cat-SAV0193-r (Table 2) were used for the amplification of a 1.5-kb region upstream of *rpiRB*, and a 1.5-kb region of the *rpiRB* downstream region was amplified using primers cat-SAV0193-f and SacI-SAV0195-r (Table 2). The *cat* gene was amplified from pTS1 using primers SAV0193-cat-f and SAV0193-cat-r (Table 2). The resulting 3.9-kb PCR product consisted of an internal 816-bp *cat* gene with DNA flanking the *rpiRB* gene. The 3.9-kb PCR product contained BamHI and SacI sites that were used for ligation into pTS1-d digested with SacI and BamHI to generate pYM-4. Plasmid pYM-4 was used to construct an *rpiRB* mutant (UAMS-1-*rpiRB::cat*) by using the temperature shift method of Foster (11).

Gene splicing by overlap extension was used to replace a 614-bp internal region of *rpiRC* (ORF SAV2315) with the *tetM* gene from plasmid pJF-12 (Table 1). A 1.5-kb region upstream of *rpiRC* was amplified using primers BamHI-SAV2312-f and tetM-SAV2315-r (Table 2), and primers tetM-SAV2315-f and KpnI-SAV2316-r (Table 2) were used for amplification of a 1.6-kb downstream region. *tetM* was amplified from pJF-12 using primers SAV2315-tetM-f and SAV2315-tetM-r (Table 2). A 5.4-kb PCR product consisting of the 2.3-kb *tetM* gene and DNA flanking the *rpiRC* gene with BamHI and KpnI sites was inserted into pTS1-d digested with BamHI and KpnI to generate pYM-5. Plasmid pYM-5 was used to construct a strain UAMS-1 *rpiRC* mutant (UAMS-1-*rpiRC::tetM*) by using temperature shifts. To minimize the possibility that any phenotype(s) was the result of random mutations occurring during temperature shifts, all resulting mutations were back-crossed into wild-type strain UAMS-1 using transducing phage ϕ85 (11). All mutants were verified by PCR and Southern blot analysis. The *rpiR* double mutants and triple mutant were constructed using transducing phage ϕ85.

Construction of *rpiR* complementing plasmids. Plasmids pCL15 and pCL15-*ermB* (Table 1), containing a P_{spac} promoter, were used to construct the *rpiRA*,

TABLE 2. Primers used in this study

Primer target	Primer designation	Nucleotide sequence (5′–3′)
SAV0317	SAV0316-BamHI	GCTGGATCCCGACTGAACAATGAACGCCTAAGTC
	SAV0318-SacI	CCTGAGCTCATCAACGCCGGACAACAAAAGTG
ermB	pEC4ErmBNdeI-f	GCGCATATGCGTTAGATTAATTCCTACCAGTGAC
	pEC4ErmBNdeI-r	GCGCATATGCTCATAGAATTATTTCCTCCCG
SAV0193	BamHI-SAV0192-f	CCAGGATCCAGAACGAATTATTGCTGCAGTAGG
	cat-SAV0193-r	CCACTTTATCCAATTTTCGTTTGTTGTTCACCGTCATATCAATGATTTTATGTGG
cat	SAV0193-cat-f	CCACATAAAATCATTGATATGACGGTGAACAACAAACGAAAATTGGATAAAGTGGG
	SAV0193-cat-r	GCAAGATGCTTCCGGTAATTATCAAGCGACTGTAAAAAGTACAGTCGGC
SAV0193	cat-SAV0193-f	GCCGACTGTACTTTTTACAGTCGCTTGATAATTACCGGAAGCATCTTGC
	SacI-SAV0195-r	GCAGAGCTCGTTGAATAAGTGCTTCTACCGCATAC
SAV2315	BamHI-SAV2312-f	CCAGGATCCGATTCCTAAACTATGGAGTCGATGGG
	tetM-SAV2315-r	CGTAAGAGCATATTTGTAAAGGAATCTCCGAGACCTCATTTTAATCACCTTTTGAGG
tetM	SAV2315-tetM-f	CCTCAAAAGGTGATTAAAATGAGGTCTCGGAGATTCCTTTACAAATATGCTCTTACG
	SAV2315-tetM-r	GAAGTTGTTGCTCCCATATGCATCCGATCTCCTCCTTTCCACTTTAATTC
SAV2315	tetM-SAV2315-f	GAATTAAAGTGGAAAGGAGGAGATCGGATGCATATGGGAGCAACAACTTC
	KpnI-SAV2316-r	GAAGGTACCAATGGATTGTAGTTGGTATGAGTGAG
RNAIII	SARNAIII-f	GAAGGAGTGATTTCAATGGCACAAG
	SARNAIII-r	GGCTCACGACCATACTTATTATTAAGGG
rpiA	rpiaf	GTGACATGACGCTGGGAATTGG
	rpiar	GTATCCTGTCTCAAACACACCTGTCAG
SAV1505	SAV1505f	GCACCACAATTCTTTGGCGTTATTTC
	SAV1505r	AGTACGAATATAGAATGGTACACCAGCC
SAV0317	BamHI-SD-rpiR-f	CAAGGATCCATTAAGATGAAGGGGTGACACAATG
	SacI-rpiR-r	CAAGAGCTCAATCACGATGATTGTCTACAGTTGC
SAV0193	BamHI-SAV0193-f	CTAGGATCCATGACAAATATTTTATATCGCATTGATAAACAGTTGAG
	SAV0193-r	CAAACAACTGAATCACATCAAAAACTTCAATTG
SAV2315	BamHI-SAV2315-f	CTAGGATCCATGTCAAACGTACTAACAGAAATAGATAGTCAATATCC
	SAV2315-r	GCGTATGTTATACAAGATAAAAGACATGTAAGCTTTG

rpiRB, and *rpiRC* complementation plasmids pYF-10, pYF-11, and pYF-12. The promoterless genes from *S. aureus* strain UAMS-1 were PCR amplified using the primers listed in Table 2 and were ligated into plasmid pCL15 or pCL15-*ermB*. Plasmids were isolated from *S. aureus* strain RN4220 and were electroporated into the UAMS-1 *rpiRA*, *rpiRB*, and *rpiRC* mutants.

Northern blot analysis. To determine whether *rpiR* inactivation affected the transcription of PPP genes, Northern blot analysis was performed on ribose 5-phosphate isomerase A (*rpiA*) and glucose-6-dehydrogenase (G6PD) (*zwf*; ORF SAV1505). RNAIII transcript levels were also evaluated in order to determine the effect of *rpiR* inactivation on the *agr* system. Northern blotting was performed as described previously (36), except that total RNA was isolated using the FastRNA Pro Blue kit (Qbiogene) and was purified using an RNeasy kit (Qiagen). Probes for Northern blotting were generated by PCR amplification of unique internal regions of RNAIII, *rpiA*, and *zwf* (Table 2) and were labeled using the North2South random prime labeling kit (Pierce). Detection was performed using the chemiluminescent nucleic acid detection module (Pierce).

Glucose-6-dehydrogenase activity assay. To determine whether *rpiR* inactivation affected PPP activity, G6PD activity was measured as described previously (7). Protein concentrations were determined using a modified Lowry assay (Pierce Chemical).

Western blot analysis. To determine whether *rpiR* inactivation affected protein A biosynthesis, protein A was collected as described previously (45), and Western blot analysis was performed (43).

Hemolytic assay. Strain UAMS-1 is lysogenized with an *hlb*-converting phage and has a nonsense mutation in *hla*; hence, it does not produce the major hemolysins alpha-toxin and beta-toxin (4). The mRNA for delta-toxin is contained within RNAIII (16). To determine whether inactivation of any *rpiR* homologue altered delta-toxin accumulation, a semiquantitative microtiter plate assay was carried out as described previously (10). Briefly, horse red blood cells (RBCs; Colorado Serum Company) were washed three times in phosphate-buffered saline (PBS) (pH 7.2) and were suspended at 2% (vol/vol) in PBS. Bacteria were grown in TSB for 15 h and were then centrifuged at 16,100 $\times$ *g* for 5 min; supernatants were collected, and 2-fold serial dilutions were made in PBS. Hemolytic assays were started by mixing 100 μl of freshly prepared 2% horse RBCs with 100 μl of serial 2-fold dilutions of the appropriate culture supernatant. The microtiter plates were incubated at 37°C for 30 min, followed by 12 h at 4°C. After incubation, the supernatant fluids were collected, and hemoglobin release was measured at 595 nm. Each experiment was repeated three times, and the mean and standard error of the mean (SEM) were calculated.

Polystyrene primary attachment assay. The primary attachment assay was performed as described by Lim et al. (19). Briefly, bacterial cultures (2 h post-inoculation) were diluted into TSB to yield approximately 300 CFU. Bacteria were poured onto polystyrene petri dishes (Fisher Scientific) and were incubated at 37°C for 30 min. Following incubation, the petri dishes were rinsed three times with sterile PBS (pH 7.5) and were covered with 15 ml of TSB containing 0.8% agar maintained at 48°C. The percentage of bacteria attached to the polystyrene was defined as the number of CFU remaining in the petri dishes after washing compared to the number of CFU in unwashed TSB plates. The experiment was repeated three times, and the mean and SEM were calculated.

Capsule immunoblot assay. To determine whether *rpiR* inactivation altered capsule biosynthesis, capsule accumulation was quantified by immunoblotting as described previously (22), except that immunoblots were developed using a chemiluminescent horseradish peroxidase (HRP) substrate (Millipore). For the capsule blots, bacteria (1.25 optical density at 660 nm [OD_{660}] units) were harvested after overnight growth in tryptic soy broth at 37°C, with a flask-to-medium ratio of 20:1, and were aerated at 225 rpm.

PIA immunoblot assay. PIA accumulation was determined after 2, 4, and 6 h of growth as described previously (47).

Biofilm formation in flow cell chambers. *S. aureus* strains were grown in flow cell chambers (Stovall Life Science) as described previously (47). To assess bacterial growth, at 12 h postinoculation and every 4 h thereafter, effluent samples were collected, the pH was measured, and the chamber was photographed.

Proteomic analyses. Bacterial cells (2 h and 6 h postinoculation) were harvested by centrifugation and were suspended in 1.0 ml of lysis buffer containing 50 mM ammonium bicarbonate, 8 M urea, and 1.5 mM phenylmethylsulfonyl fluoride (PMSF). The samples were homogenized for 40 s at 6.0 m/s in a FastPrep instrument (MP Biomedical), and the lysate was centrifuged for 5 min at 20,800 × *g* and 4°C. Bacterial proteins were subjected to in-solution trypsin digestion as described previously (28). Briefly, the proteins were reduced with 10 mM dithiothreitol and were alkylated with 40 mM iodoacetamide, followed by trypsin (Roche) digestion (trypsin/protein ratio, 1:50) overnight at 37°C. The tryptic peptides were desalted and concentrated using PepClean C_{18} spin columns according to the manufacturer's instructions (Thermo Scientific).

Fully automated 2-dimensional (2D) chromatographic experiments were performed with an UltiMate 3000 Proteomics multidimensional liquid chromatography (MDLC) system (Dionex Corporation) integrated with a nanospray source and an LCQ (liquid chromatography quadrupole) Fleet ion trap mass spectrometer (Thermo Scientific). The first-dimension LC separation (strong cation-exchange [SCX] chromatography) with fraction collection was followed by the second-dimension LC separation (reverse-phase chromatography) and detection by tandem mass spectrometry (MS-MS). The first-dimension separation was performed on an SCX column (polysulfoethyl; inside diameter [i.d.], 1 mm; length, 15 cm; particle size, 5 μm; pore size, 300 Å; Dionex). Twenty microliters of the sample was loaded onto the first-dimension SCX column and was eluted using a salt gradient (0 to 600 mM) for 45 min. Based on the UV absorbance of the eluted peptides, selected fractions were subjected to second-dimension analysis. The second-dimension separation included on-line sample preconcentration and desalting using a monolithic C_{18} trap column (PepMap; i.d., 300 μm; length, 5 mm; particle size, 5 μm; pore size, 100 Å; Dionex). The sample was loaded onto the monolithic trap column at a flow rate of 300 nl/min. The desalted peptides were then eluted and separated on a C_{18} PepMap column (i.d., 75 μm; length, 15 cm; particle size, 3 μm; pore size, 100 Å) by applying an acetonitrile (ACN) gradient (ACN plus 0.1% formic acid; 90-min gradient at a flow rate of 300 nl/min) and were introduced into the mass spectrometer using the nanospray source. The LCQ Fleet mass spectrometer was operated with the following parameters: nanospray voltage, 2.0 kV; heated capillary temperature, 200°C; full-scan *m/z* range, 400 to 2,000. The mass spectrometer was operated in the data-dependent mode with 4 MS-MS spectra for every full scan, 5 microscans averaged for full scans and MS-MS scans, a 3 *m/z* isolation width for MS-MS isolations, and 35% collision energy for collision-induced dissociation.

The MS-MS spectra were searched against the *S. aureus* MRSA252 database using MASCOT (version 2.2; Matrix Science). The database search criteria were as follows: enzyme, trypsin; missed cleavages, 2; mass, monoisotropic; fixed modification, carbamidomethyl (C); peptide tolerance, 1.5 Da; MS-MS fragment ion tolerance, 1 Da. Probability assessment of peptide assignments and protein identifications were accomplished by Scaffold (version 3.0; Proteome Software Inc.). Only peptides with ≥90% probability were considered. Criteria for protein identification included the detection of at least 2 unique identified peptides and a protein probability score of ≥90%. Relative quantitation of proteins was done by use of the label-free method of spectral counting (20) using the normalized spectral counts for each protein. For ease of reference, the NCBI GenInfo Identifier (gi) numbers have been included in this report and in Tables S1 and S2 in the supplemental material.

Hydrogen peroxide susceptibility assay. To determine if *rpiR* inactivation affects hydrogen peroxide susceptibility, *S. aureus* strain UAMS-1 and all of the *rpiR* mutant strains were grown in TSB for 15 h and were then diluted to an OD_{600} of 0.05 into sterile medium containing increasing concentrations of hydrogen peroxide (Fisher Scientific). Cultures were grown at 37°C with shaking (225 rpm) for 4 h. Bacterial densities were determined by measuring the OD_{600}.

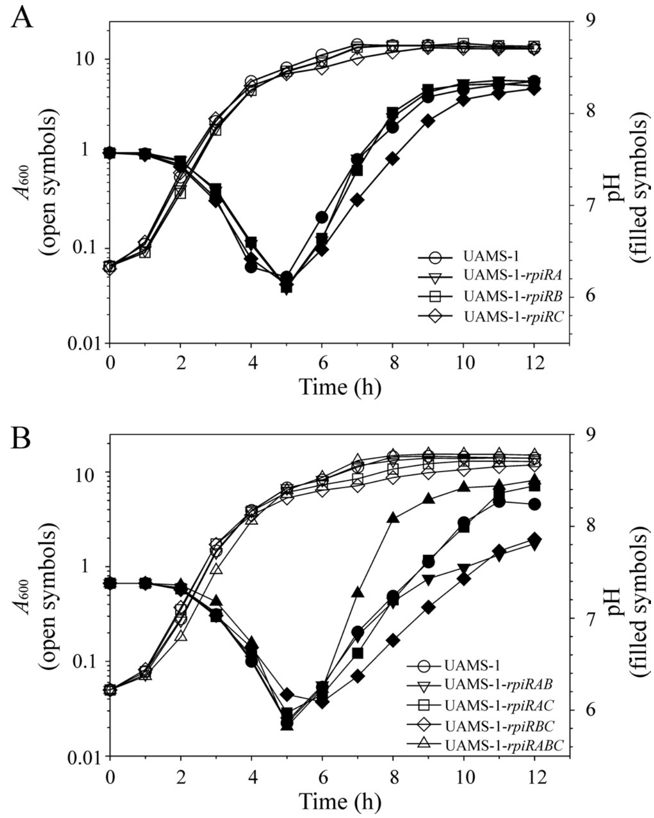

FIG. 1. Deletion of any *rpiR* homologue in strain UAMS-1 does not alter the growth profile in TSB medium. (A) Growth curves and culture medium pH profiles are shown for strain UAMS-1 and for the UAMS-1-*rpiRA*, UAMS-1-*rpiRB*, and UAMS-1-*rpiRC* mutants (A) and the UAMS-1-*rpiRAB*, UAMS-1-*rpiRAC*, UAMS-1-*rpiRBC*, and UAMS-1-*rpiRABC* mutants (B).

RESULTS

Characterization of *rpiR* mutants. Analysis of the Mu50 genome (18) revealed the presence of three RpiR homologues: RpiRA (SAV0317), RpiRB (SAV0193), and RpiRC (SAV2315). Each *rpiR* homologue was deleted either individually or in tandem with one or both of the other *rpiR* homologues in strain UAMS-1 (Table 1). To assess the effects of inactivation of the *rpiR* homologue genes on growth, the optical densities and pH of the culture medium (TSB) were measured over time (Fig. 1). Inactivation of any single *rpiR* homologue in UAMS-1 did not alter the growth rate, growth yield, or pH profile of the culture medium (Fig. 1A). Similarly, the double and triple mutants had growth rates and growth yields equivalent to those of the wild-type strain UAMS-1 (Fig. 1B). Of note, the pH profile of the culture medium for the triple mutant showed an increased rate of alkalization relative to that for the wild-type strain, suggesting that this strain had an increased rate of acetic acid utilization or an increase in ammonia generation due to amino acid catabolism (Fig. 1B). These results demonstrate that the growth of the *rpiR* mutants is equivalent to that of the isogenic wild-type strain.

RpiR homologues regulate PPP activity. As stated above, RpiR was first identified in *E. coli* as a repressor of the PPP gene *rpiB* (42). Similarly, the *Pseudomonas putida* RpiR ho-

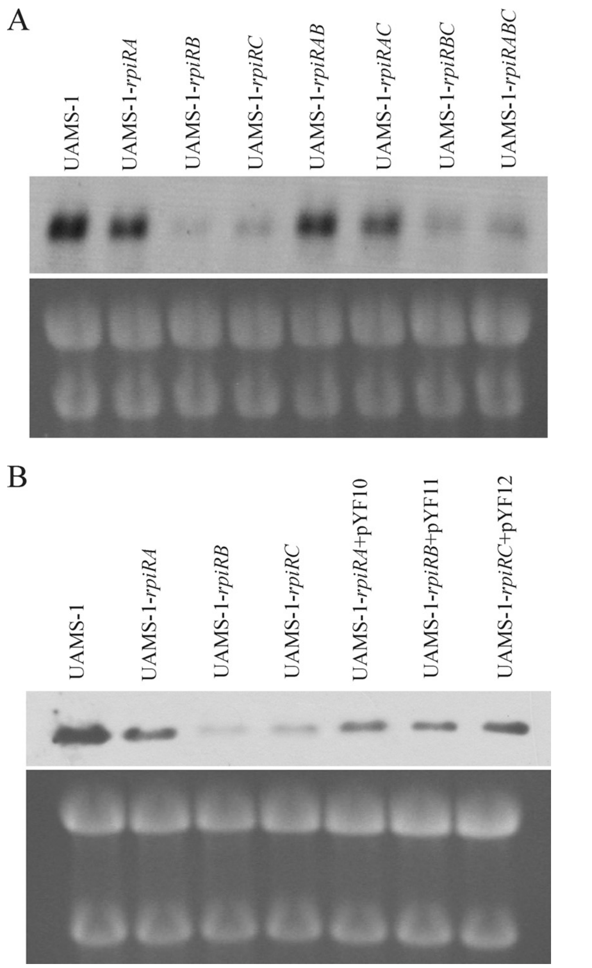

FIG. 2. Inactivation of *rpiR* homologues alters *rpiA* mRNA accumulation. (A) Northern blot analysis demonstrating that inactivation of *rpiRB* or *rpiRC* decreases the transcription of ribose phosphate isomerase A (*rpiA*). (B) Northern blot analysis demonstrating that complementation of *rpiRB* or *rpiRC* restores *rpiA* transcription. Ethidium bromide-stained agarose gels showing 23S and 16S rRNA are included in each panel to demonstrate the equivalent loading of total RNA. The results are representative of at least two independent experiments.

mologue HexR regulates *zwf*, which codes for glucose 6-phosphate dehydrogenase (G6PD), the rate-controlling enzyme of the PPP (8). These data led us to hypothesize that one or more of the RpiR homologues in *S. aureus* would regulate the transcription of PPP genes. To test this hypothesis, transcription of the PPP genes *rpiA* (ribose-5-phosphate isomerase A) and *zwf* (*sav1505*; coding for G6PD) in the *rpiR* mutant strains was assessed by Northern blot analysis of total RNA isolated during the exponential phase of growth (2 h) (Fig. 2A and data not shown). Deletion of *rpiRB* or *rpiRC* decreased the transcription of both *rpiA* and *zwf* relative to that in the parental strain UAMS-1; however, *rpiRA* inactivation had only a minor effect on *rpiA* and *zwf* mRNA levels (Fig. 2A and data not shown). Complementation of the UAMS-1 *rpiRB* and *rpiRC* mutants increased the levels of *rpiA* mRNA (Fig. 2B), confirming that the transcriptional changes are due to the inactivation of the mutated *rpiR* genes. Interestingly, deletion of *rpiRA* in either an *rpiRB* or an *rpiRC* mutant strain restored the level of *rpiA* mRNA to that found in strain UAMS-1 (Fig. 2A), suggesting an antagonistic effect between RpiRA and both RpiRB and RpiRC. Because *zwf* mRNA migrates on an agarose gel near rRNA, and in order to confirm the Northern blot data, the activity of G6PD was assessed in the wild-type and *rpiR* mutant strains. In agreement with the Northern blot data, mutation of *rpiRB* or *rpiRC* led to decreased G6PD enzymatic activity in the exponential-growth phase (2 h) (see Fig. S1 in the supplemental material) relative to that for the wild-type strain UAMS-1. Also consistent with the Northern blot data are the antagonistic effects of RpiRA on G6PD activity in both the *rpiRB* and *rpiRC* mutant backgrounds. In contrast to the findings for the exponential-growth phase, only *rpiRB* inactivation significantly decreased G6PD enzymatic activity during the post-exponential-growth phase (8 h) relative to that for the wild-type strain (see Fig. S1). Overall, these data demonstrated that RpiRB and RpiRC have a positive regulatory function in PPP regulation and that RpiRA is antagonistic to this function.

Inactivation of *rpiRC* delays biofilm development and decreases the synthesis of cell wall-associated virulence determinants. Nuclear magnetic resonance (NMR) metabolomic analysis indicated that the intracellular ribose concentration in *S. epidermidis* changes in response to stressors that induce biofilm formation and PIA accumulation (35). Because the RpiR homologues have been reported to respond to PPP intermediates in other bacteria (8), we assessed the effects of *rpiR* inactivation on biofilm formation and PIA accumulation (Fig. 3A and data not shown). The deletion of any *rpiR* homologue, singly or in tandem, did not significantly alter the accumulation of PIA (data not shown). In *S. aureus*, biofilms can form in the absence of PIA biosynthesis (2); therefore, the lack of any significant effect of *rpiR* inactivation on PIA accumulation did not preclude the possibility that one or more of the RpiR homologues would affect biofilm formation. Consistent with this premise, deletion of *rpiRC* delayed biofilm maturation (Fig. 3A). While biofilm maturation was delayed, the gross morphologies of the biofilms formed by the wild-type and *rpiRC* mutant strains were similar after 24 h of growth. The delay in biofilm maturation and the absence of any attenuation of PIA accumulation were consistent with a defect in bacterial attachment or adhesion. To determine whether inactivation of *rpiRC* decreased adhesin synthesis, polystyrene attachment assays were used to assess the abilities of wild-type and *rpiR* mutant strains to adhere to surfaces (Fig. 3B). In agreement with the delay in biofilm formation, strains containing a mutation in *rpiRC* had a significantly decreased ability to attach to polystyrene relative to that of the parental strain (Fig. 3B). Taken together, these data suggest that the synthesis of cell wall-associated adhesins was decreased by *rpiRC* inactivation.

The association of protein A with biofilm formation (26) and the decreased ability of *rpiR* mutant strains to adhere to polystyrene suggested that cell-associated adhesin synthesis was impaired by inactivation of one or more RpiR homologues. Protein A is synthesized primarily during the exponential-growth phase and is considered representative of cell wall-associated protein synthesis. To determine whether *rpiR* inactivation altered the exponential-growth-phase expression of protein A and potentially of other cell wall-associated proteins, the exponential-growth-phase accumulation of protein A was

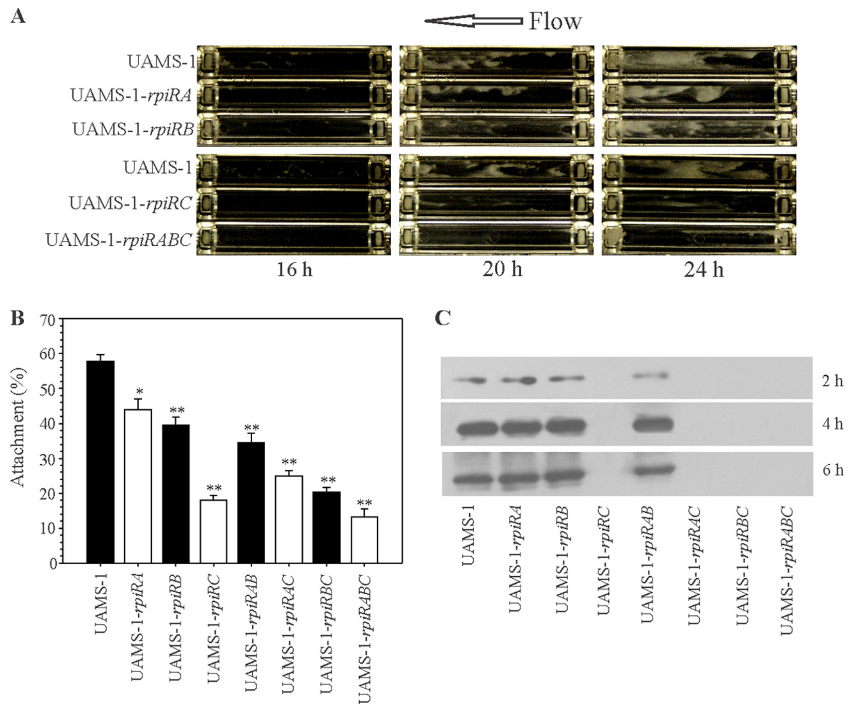

FIG. 3. Deletion of *rpiRC* delays biofilm maturation by inhibiting adhesion and the synthesis of cell-associated virulence determinants. (A) Growth of *S. aureus* strains UAMS-1, UAMS-1-*rpiRA*, UAMS-1-*rpiRB*, UAMS-1-*rpiRC*, and UAMS-1-*rpiRABC* in three-chamber flow cells. Bacterial strains were grown at 37°C with a continuous flow (0.5 ml min^{-1} per chamber) of TSB containing 0.5% glucose and 3% NaCl. The results are representative of at least two independent experiments. (B) Adhesion of *S. aureus* strains to polystyrene. The data are presented as means and SEMs for three independent experiments. Significant differences, as determined using Student's *t* test, are indicated by asterisks (**, $P < 0.01$; *, $P < 0.05$). (C) Western blot analysis of protein A. The blot is representative of three independent experiments.

assessed by Western blotting (Fig. 3C). Mutations in either *rpiRA* or *rpiRB* did not affect the accumulation of protein A relative to that for strain UAMS-1; however, inactivation of *rpiRC* completely inhibited the exponential-growth-phase accumulation of protein A (Fig. 3C). Interestingly, *rpiRA* inactivation did not antagonize the expression of protein A in the *rpiRC* mutant background, suggesting that the antagonistic effects of RpiRA are confined to regulation of the PPP. In total, these data suggest that RpiRC acts as a regulatory bridge between the PPP and virulence factor synthesis in *S. aureus*.

RpiRC represses RNAIII transcription or message stability. RNAIII is the effector RNA of the *agr* quorum-sensing system and a negative regulator of protein A (*spa*) (29). Mutation of *rpiRC* eliminated the exponential-growth-phase accumulation of protein A (Fig. 3C), raising the possibility that RNAIII transcription or stability was increased. To determine whether *rpiR* inactivation affected RNAIII levels, Northern blot analysis of RNAIII was performed on all *rpiR* mutant strains throughout a 12-h growth cycle (Fig. 4A and B). As expected, *rpiRC* inactivation increased the RNAIII transcript level relative to that for the parental strain during the exponential-growth phase (2 h) (Fig. 4A). Complementation of the *rpiRC* mutation with pYF-12 decreased the level of RNAIII relative to that for the *rpiRC* mutant strain, confirming that the increased RNAIII level was due to *rpiRC* inactivation (Fig. 4B). In agreement with the results of the Western blot analysis of protein A and the attachment assays (Fig. 3B and C), we did not observe an antagonistic effect of *rpiRA* inactivation on the exponential-growth-phase (2 h) transcription or stability of RNAIII in either an *rpiRB* or an *rpiRC* mutant background (Fig. 4A). Although RNAIII levels were largely independent of RpiRA or RpiRB in the exponential-growth phase, *rpiRB* inactivation increased the post-exponential-growth-phase RNAIII transcript levels (Fig. 4B). RNAIII is both a riboregulator and the coding sequence for delta-toxin (16); therefore, if RNAIII levels are increased, it is likely that delta-toxin synthesis is increased. (Strain UAMS-1 is lysogenized with an *hlb*-converting phage and has a nonsense mutation in *hla*; hence, it does not produce the major hemolysins alpha-toxin and beta-toxin [4].) By use of a hemolytic titer assay, the increased RNAIII levels correlated with an increase in hemolysis activity (Fig. 5A). In total, these data indicate that RpiRC represses RNAIII transcription during the exponential-growth phase, while RpiRB represses RNAIII transcription during the post-exponential-growth phase.

In *S. aureus*, strain-dependent differences in the regulation of virulence determinant biosynthesis have been reported (4, 49). To determine whether the effect of RpiR inactivation on RNAIII transcription was common to *S. aureus* strains from divergent genetic backgrounds, the *rpiRB* and *rpiRC* mutations were transduced into *S. aureus* strain SA564 (38), and Northern blot analysis of RNAIII was performed (see Fig. S2 in the supplemental material). As with strain UAMS-1, inactivation of *rpiRC* in strain SA564 derepressed RNAIII transcription during the exponential-growth phase and had no effect during

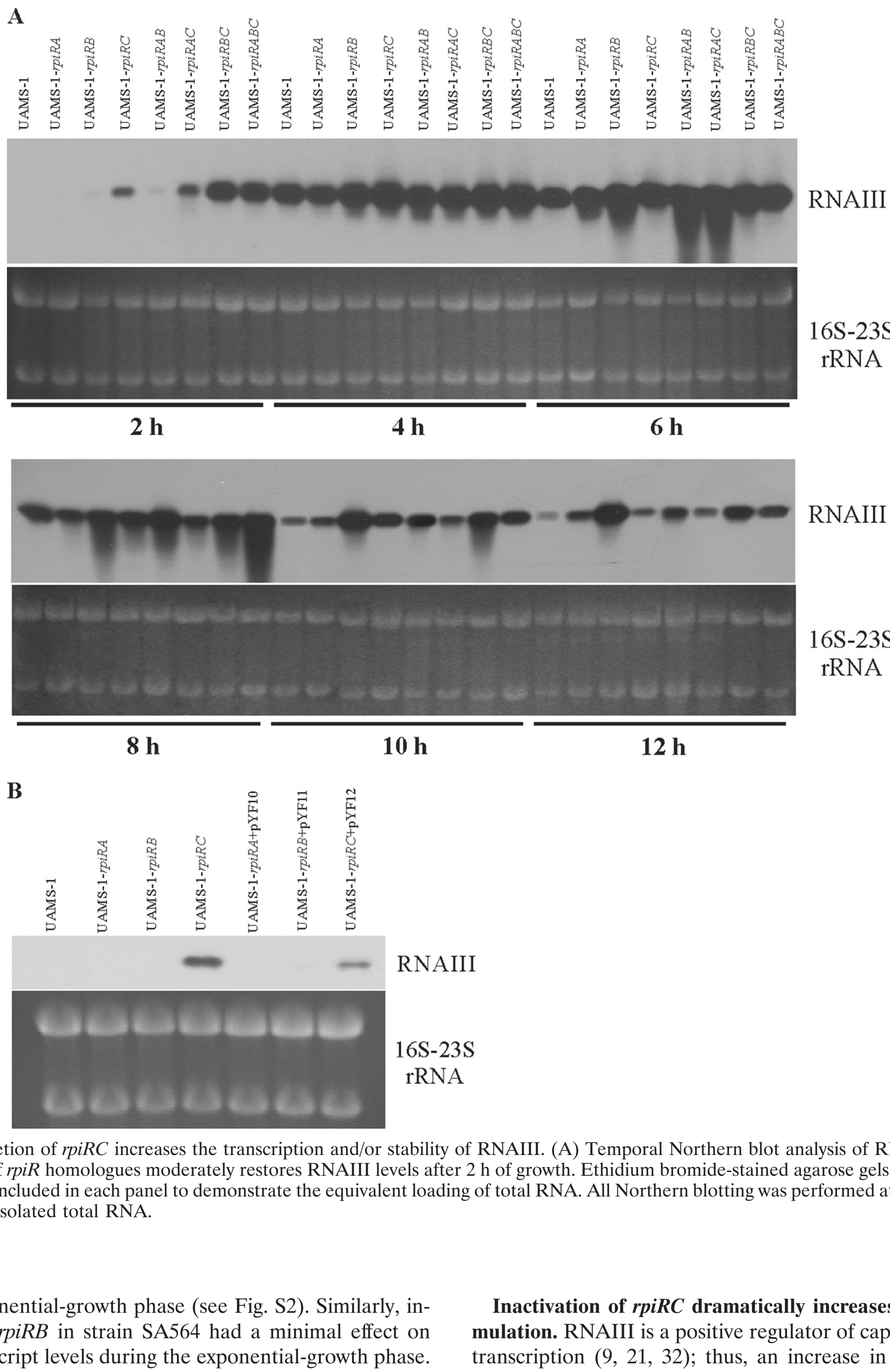

FIG. 4. Deletion of *rpiRC* increases the transcription and/or stability of RNAIII. (A) Temporal Northern blot analysis of RNAIII. (B) Complementation of *rpiR* homologues moderately restores RNAIII levels after 2 h of growth. Ethidium bromide-stained agarose gels showing 23S and 16S rRNA are included in each panel to demonstrate the equivalent loading of total RNA. All Northern blotting was performed at least twice using independently isolated total RNA.

the post-exponential-growth phase (see Fig. S2). Similarly, inactivation of *rpiRB* in strain SA564 had a minimal effect on RNAIII transcript levels during the exponential-growth phase. In contrast to the finding for strain UAMS-1, inactivation of *rpiRB* in strain SA564 had no apparent effect on RNAIII transcription during the post-exponential-growth phase. These data demonstrate that RpiRC represses the exponential-growth-phase level of RNAIII in divergent genetic backgrounds.

Inactivation of *rpiRC* dramatically increases capsule accumulation. RNAIII is a positive regulator of capsule gene (*cap*) transcription (9, 21, 32); thus, an increase in RNAIII levels should correlate with an increase in capsule biosynthesis. To determine whether *rpiR* inactivation affects capsule biosynthesis, capsule accumulation was assessed by capsule immunoblotting. In agreement with the increased RNAIII levels, inactivation of all three *rpiR* genes increased capsule accumulation (Fig. 5B); however, the increased accumulation of capsule was

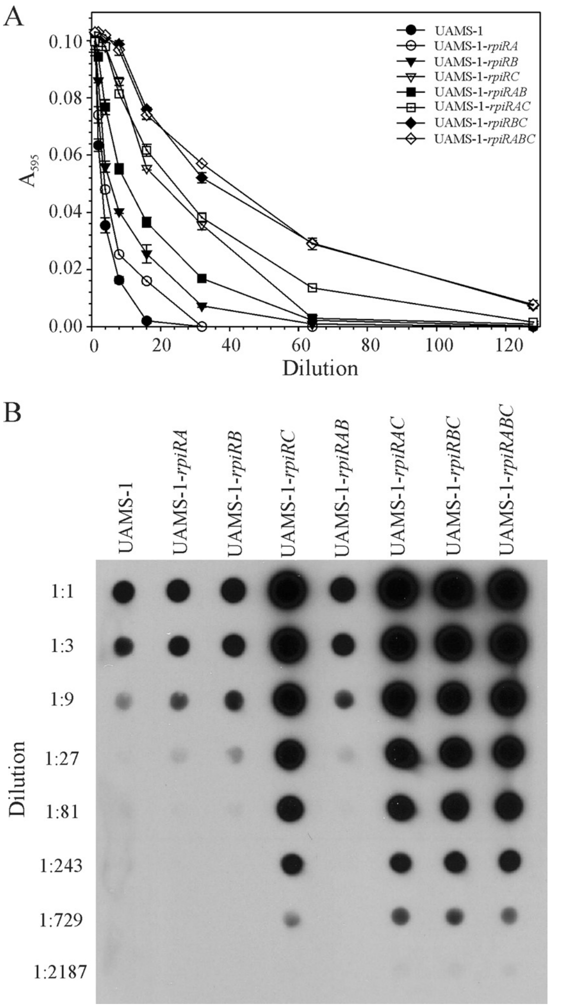

FIG. 5. Inactivation of *rpiR* homologues alters virulence factor synthesis. (A) Hemolytic activities of culture supernatants from strain UAMS-1 and the *rpiR* mutant strains against washed rabbit erythrocytes. The data are presented as the means and SEMs for three independent experiments. (B) Immunoblotting for capsule polysaccharide. The blot is representative of at least two independent experiments.

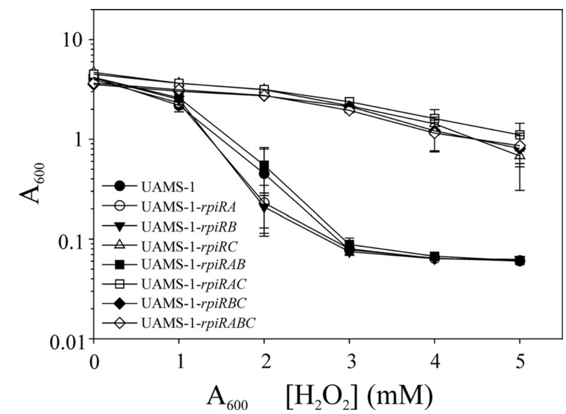

FIG. 6. Deletion of *rpiRC* decreases the susceptibility of *S. aureus* strains to hydrogen peroxide. Data are presented as the means and SEMs for three independent experiments.

most apparent in strains with a mutation in *rpiRC*. These data strongly suggest that the RpiR-dependent derepression of RNAIII facilitates virulence determinant expression and that the RpiR proteins act as a bridge between the PPP and virulence factor synthesis.

Inactivation of *rpiRC* alters the proteome. To identify changes in cytosolic protein content in strain UAMS-1 and the *rpiRC* mutant strains, cell-free lysates were prepared from strains UAMS-1, UAMS-1-*rpiRC*, and UAMS-1-*rpiRABC* grown to the exponential and post-exponential phases of growth and were analyzed by 2D LC–MS-MS (see Tables S1 and S2 in the supplemental material). Although *rpiRC* inactivation resulted in numerous proteomic changes, we were specifically interested in changes to PPP enzymes and proteins that might clarify the increased RNAIII transcript levels. Proteomic analysis showed that the PPP enzymes transaldolase (gi|49242155) and ribose-phosphate pyrophosphokinase (gi|49240856) were present at lower concentrations in strains UAMS-1-*rpiRC* and UAMS-1-*rpiRABC* than in strain UAMS-1, consistent with regulation of the PPP by RpiRC. Interestingly, deletion of *rpiRC* increased the accumulation of ribosomal proteins (see Tables S1 and S2 in the supplemental material); however, the reason for this remains unknown. Proteomic analysis also suggested that there was an increase in the levels of proteins associated with σ^B; specifically, inactivation of *rpiRC* increased the concentrations of the alkaline shock protein A (Asp23; gi|49242531) and RsbU (gi|49242422) (see Tables S1 and S2). Because *asp23* transcription is controlled exclusively by σ^B, Asp23 is used as an indicator of σ^B activity (17, 27). RsbU is a phosphatase that dephosphorylates (activates) the anti-anti-sigma factor RsbV, which then binds the anti-sigma factor RsbW in a competitive manner to increase the concentration of free σ^B (12). In addition to regulating the transcription of *asp23*, σ^B regulates the transcription of *sarA* from the *sar* P3 promoter (27). SarA is a positive effector of *agrACDB* and RNAIII transcription (5). Inactivation of *rpiRC* increased RNAIII levels relative to those in the wild-type strain (Fig. 4), suggesting that *rpiRC* inactivation might increase the availability of SarA. Consistent with this suggestion, *rpiRC* inactivation increased the cytosolic concentration of SarA (gi|49240975) during both the exponential- and post-exponential-growth phases (see Tables S1 and S2). These data suggest that the increased RNAIII levels in the *rpiRC* mutants are due to increased availability of σ^B, which increases *sarA* transcription and translation, resulting in increased RNAIII transcription.

Inactivation of *rpiRC* decreases peroxide susceptibility. In some strains of *S. aureus*, σ^B has been implicated in susceptibility to oxidative stress (12, 17). This observation and the fact that strain UAMS-1-*rpiRC* had higher ferritin and catalase levels than strain UAMS-1 (see Tables S1 and S2 in the supplemental material) led us to assess the susceptibilities of strain UAMS-1 and the *rpiR* mutants to peroxide stress (Fig. 6). As expected, inactivation of *rpiRC* significantly decreased the susceptibilities of strains UAMS-1-*rpiRC*, UAMS-1-*rpiRAC*, UAMS-1-*rpiRBC*, and UAMS-1-*rpiRABC* to hydrogen peroxide relative to that of strain UAMS-1 (Fig. 6). Taken together, these data demonstrate that the *S. aureus* RpiR family of proteins functions in cell survival under conditions of oxidative stress.

DISCUSSION

Three central metabolic pathways (i.e., glycolysis, the PPP, and the TCA cycle) provide the 13 biosynthetic intermediates needed to synthesize all macromolecules produced in bacteria. By default, virulence determinants are synthesized from these 13 biosynthetic intermediates of central metabolism; hence, virulence determinant synthesis is dependent on the endogenous or exogenous availability of these intermediates or byproducts of these intermediates. Because of the importance of these intermediates, bacteria have evolved metabolite-responsive regulators (e.g., CcpA, CodY) that "sense" the availability of these intermediates or compounds derived from them (41). Not only do these metabolite-responsive regulators function to maintain metabolic homeostasis; many also regulate virulence determinant synthesis (41). Although metabolite-responsive regulators that respond to changes in the levels of glycolytic and TCA cycle intermediates or derivatives have been identified in *S. aureus*, none that respond to changes in the levels of PPP intermediates have been identified. To that end, three RpiR family members, RpiRA, RpiRB, and RpiRC, were identified and inactivated in *S. aureus* strain UAMS-1, and the phenotypic and regulatory changes associated with each RpiR homologue were characterized.

PPP regulation. RpiRB and RpiRC positively regulate the exponential-growth-phase transcription of the PPP genes *rpiA* and *zwf* (Fig. 2A). In addition, RpiRC positively affects the expression of transaldolase and ribose-phosphate pyrophosphokinase (see Tables S1 and S2 in the supplemental material). Although RpiRB and RpiRC are paralogues, there appears to be minimal overlap in function between the two regulatory proteins, since inactivation of either *rpiRB* or *rpiRC* decreases the transcription of *rpiA* and *zwf* to the same extent (Fig. 2A). In other words, RpiRB does not compensate for the loss of RpiRC, and RpiRC does not compensate for the loss of RpiRB. Interestingly, RpiRA has only a slight effect on *rpiA* and *zwf* transcription; however, it does antagonize the regulatory effects of both RpiRB and RpiRC (Fig. 2A). In double mutants, inactivation of *rpiRA* restores the transcription of *rpiA* and, to a lesser extent, *zwf* to near-wild-type levels. Interestingly, this antagonism involves only RpiRB- and RpiRC-dependent regulation of *rpiA* and *zwf*, not RpiRC-dependent regulation of RNAIII (Fig. 4A and B). Taken together, these data confirm that the *S. aureus* RpiR homologues positively affect PPP transcription and activity.

RNAIII regulation. Synthesis of RNAIII is under the control of the *agr* cell density-sensing system (31); hence, RNAIII transcription usually begins late in the exponential phase of growth (~4 h) (Fig. 4A). The growth rates and growth yields of the UAMS-1 *rpiRA*, *rpiRB*, and *rpiRC* mutant strains are equivalent to those of the parental strain (Fig. 1A); thus, it was surprising to find that the transcription of RNAIII was derepressed during the early-exponential-growth phase (2 h) in strain UAMS-1-*rpiRC* compared to that in strain UAMS-1 (Fig. 4A). This RpiRC-dependent derepression persists into the post-exponential-growth phase (4 to 6 h) but declines thereafter (Fig. 4A). The more likely explanations for the RpiRC-dependent derepression of RNAIII transcription are either an increase in the level of expression of the *agr* cell density-sensing system or an *agr*-independent increase in the level of RNAIII transcription. Proteomic analysis of the cytosolic fractions of strains UAMS-1, UAMS-1-*rpiRC*, and UAMS-1-*rpiRABC* (see Tables S1 and S2 in the supplemental material) demonstrated that *rpiRC* inactivation increased the intracellular SarA concentration during the exponential (2 h)- and post-exponential (6 h)-growth phases relative to that in the parental strain UAMS-1. The increased level of SarA is likely mediated by an increase in the level of free σ^B due to enhanced RsbU phosphatase activity (gi|49242422) (see Tables S1 and S2 in the supplemental material). We speculate that the increase in the level of free σ^B is a response to increased oxidative stress. This increase in oxidative stress would occur as carbon flow through glycolysis is increased due to the diversion of carbon away from the PPP. This leads to an increase in the reducing potential, which requires the oxidation of dinucleotides via the electron transport chain to maintain redox homeostasis. An increase in electron transport chain activity would result in an increase in the release of reactive oxygen species. This speculation is supported by proteomic analysis, which revealed increases in the levels of enzymes of glycolysis and the electron transport chain in the *rpiRC* and *rpiRABC* mutants relative to those in the wild-type strain. Consistent with an increase in free σ^B levels, proteomic analysis also revealed that *rpiRC* inactivation resulted in a greater accumulation of the σ^B-regulated alkaline shock protein A (gi|49242531) in strain UAMS-1-*rpiRC*. These data suggest that the increased level of RNAIII in strains lacking RpiRC is due to an increase in the SarA-mediated transcription of RNAIII. While these data form the basis for one explanation of how RpiRC can regulate virulence determinant synthesis, it is an incomplete explanation, because data regarding known regulators, such as Rot (25), were not present in the proteomic analysis. That being said, these data confirm a direct linkage between central metabolism (i.e., the PPP) and three major virulence regulators (SarA, σ^B, and RNAIII) in *S. aureus*. Finally, these data demonstrate that putative metabolite-responsive regulators can override the normal quorum-sensing-dependent temporal pattern of virulence determinant synthesis.

Conclusions. Richard Novick postulated in a "black-box" model (29) that an energy signal derived from intermediary metabolism would, in an unknown (i.e., black-box) fashion, regulate the transcription of the *agr* cell density-sensing system. Since the introduction of this black-box model, several regulators (e.g., CcpA and CodY) that link metabolism to the regulation of virulence determinants have been identified (reviewed in reference 41). In the present study, it was observed that RNAIII synthesis is coregulated with central metabolism, specifically the PPP, through the direct or indirect action of three RpiR family regulators. Although the black-box model is largely accurate, based on data presented here and in other studies (23, 24, 37), the energy signal responsible for regulating the transcription of *agr* is more than likely a carbon signal.

In *Pseudomonas putida*, the DNA binding activity of the RpiR homologue HexR is modulated by the Entner-Doudoroff pathway intermediate 2-keto-3-deoxy-6-phosphogluconate (8). The three *S. aureus* RpiR homologues all have sugar isomerase binding domains, suggesting that their regulatory activity may be controlled by intermediates of the PPP. Collaborative studies are under way to identify the metabolites to which the RpiR homologues bind; hopefully, this information will fill in one of the black boxes in *S. aureus* virulence factor regulation.

ACKNOWLEDGMENTS

This article is a contribution of the University of Nebraska Agricultural Research Division, supported in part by funds provided through the Hatch Act and the National Institutes of Health (AI087668) to G.A.S. C.Y.L. was supported by funds provided by the National Institutes of Health (AI-37027 and AI-67857).

We thank Markus Bischoff for critical review of the manuscript and helpful discussions. Additionally, we thank the reviewers for helpful suggestions.

REFERENCES

1. **Bateman, A.** 1999. The SIS domain: a phosphosugar-binding domain. Trends Biochem. Sci. **24:**94–95.
2. **Boles, B. R., M. Thoendel, A. J. Roth, and A. R. Horswill.** 2010. Identification of genes involved in polysaccharide-independent *Staphylococcus aureus* biofilm formation. PLoS One **5:**e10146.
3. **Brückner, R.** 1997. Gene replacement in *Staphylococcus carnosus* and *Staphylococcus xylosus*. FEMS Microbiol. Lett. **151:**1–8.
4. **Cassat, J., et al.** 2006. Transcriptional profiling of a *Staphylococcus aureus* clinical isolate and its isogenic *agr* and *sarA* mutants reveals global differences in comparison to the laboratory strain RN6390. Microbiology **152:** 3075–3090.
5. **Cheung, A. L., M. G. Bayer, and J. H. Heinrichs.** 1997. *sar* genetic determinants necessary for transcription of RNAII and RNAIII in the *agr* locus of *Staphylococcus aureus*. J. Bacteriol. **179:**3963–3971.
6. **Cheung, A. L., K. A. Nishina, M. P. Trotonda, and S. Tamber.** 2008. The SarA protein family of *Staphylococcus aureus*. Int. J. Biochem. Cell Biol. **40:**355–361.
7. **Clarke, P. M., and M. A. Payton.** 1983. An enzymatic assay for acetate in spent bacterial culture supernatants. Anal. Biochem. **130:**402–405.
8. **Daddaoua, A., T. Krell, and J. L. Ramos.** 2009. Regulation of glucose metabolism in *Pseudomonas*: the phosphorylative branch and Entner-Doudoroff enzymes are regulated by a repressor containing a sugar isomerase domain. J. Biol. Chem. **284:**21360–21368.
9. **Dassy, B., T. Hogan, T. J. Foster, and J. M. Fournier.** 1993. Involvement of the accessory gene regulator (*agr*) in expression of type 5 capsular polysaccharide by *Staphylococcus aureus*. J. Gen. Microbiol. **139**(Pt. 6):1301–1306.
10. **Fitzgerald, J. R., P. J. Hartigan, W. J. Meaney, and C. J. Smyth.** 2000. Molecular population and virulence factor analysis of *Staphylococcus aureus* from bovine intramammary infection. J. Appl. Microbiol. **88:**1028–1037.
11. **Foster, T. J.** 1998. Molecular genetic analysis of staphylococcal virulence. Methods Microbiol. **27:**433–454.
12. **Giachino, P., S. Engelmann, and M. Bischoff.** 2001. σ^B activity depends on RsbU in *Staphylococcus aureus*. J. Bacteriol. **183:**1843–1852.
13. **Gillaspy, A. F., et al.** 1995. Role of the accessory gene regulator (*agr*) in pathogenesis of staphylococcal osteomyelitis. Infect. Immun. **63:**3373–3380.
14. **Greene, C., et al.** 1995. Adhesion properties of mutants of *Staphylococcus aureus* defective in fibronectin-binding proteins and studies on the expression of *fnb* genes. Mol. Microbiol. **17:**1143–1152.
15. **Horton, R. M., Z. L. Cai, S. N. Ho, and L. R. Pease.** 1990. Gene splicing by overlap extension: tailor-made genes using the polymerase chain reaction. Biotechniques **8:**528–535.
16. **Janzon, L., and S. Arvidson.** 1990. The role of the delta-lysin gene (*hld*) in the regulation of virulence genes by the accessory gene regulator (*agr*) in *Staphylococcus aureus*. EMBO J. **9:**1391–1399.
17. **Kullik, I., P. Giachino, and T. Fuchs.** 1998. Deletion of the alternative sigma factor σ^B in *Staphylococcus aureus* reveals its function as a global regulator of virulence genes. J. Bacteriol. **180:**4814–4820.
18. **Kuroda, M., et al.** 2001. Whole genome sequencing of meticillin-resistant *Staphylococcus aureus*. Lancet **357:**1225–1240.
19. **Lim, Y., M. Jana, T. T. Luong, and C. Y. Lee.** 2004. Control of glucose- and NaCl-induced biofilm formation by *rbf* in *Staphylococcus aureus*. J. Bacteriol. **186:**722–729.
20. **Liu, H., R. G. Sadygov, and J. R. Yates III.** 2004. A model for random sampling and estimation of relative protein abundance in shotgun proteomics. Anal. Chem. **76:**4193–4201.
21. **Luong, T., S. Sau, M. Gomez, J. C. Lee, and C. Y. Lee.** 2002. Regulation of *Staphylococcus aureus* capsular polysaccharide expression by *agr* and *sarA*. Infect. Immun. **70:**444–450.
22. **Luong, T. T., S. W. Newell, and C. Y. Lee.** 2003. Mgr, a novel global regulator in *Staphylococcus aureus*. J. Bacteriol. **185:**3703–3710.
23. **Majerczyk, C. D., et al.** 2010. Direct targets of CodY in *Staphylococcus aureus*. J. Bacteriol. **192:**2861–2877.
24. **Majerczyk, C. D., et al.** 2008. *Staphylococcus aureus* CodY negatively regulates virulence gene expression. J. Bacteriol. **190:**2257–2265.
25. **McNamara, P. J., K. C. Milligan-Monroe, S. Khalili, and R. A. Proctor.** 2000. Identification, cloning, and initial characterization of *rot*, a locus encoding a regulator of virulence factor expression in *Staphylococcus aureus*. J. Bacteriol. **182:**3197–3203.
26. **Merino, N., et al.** 2009. Protein A-mediated multicellular behavior in *Staphylococcus aureus*. J. Bacteriol. **191:**832–843.
27. **Miyazaki, E., J. M. Chen, C. Ko, and W. R. Bishai.** 1999. The *Staphylococcus aureus rsbW* (orf159) gene encodes an anti-sigma factor of SigB. J. Bacteriol. **181:**2846–2851.
28. **Nandakumar, R., C. Espirito Santo, N. Madayiputhiya, and G. Grass.** 2011. Quantitative proteomic profiling of the *Escherichia coli* response to metallic copper surfaces. Biometals **24:**429–444.
29. **Novick, R. P.** 2003. Autoinduction and signal transduction in the regulation of staphylococcal virulence. Mol. Microbiol. **48:**1429–1449.
30. **Novick, R. P.** 1991. Genetic systems in staphylococci. Methods Enzymol. **204:**587–636.
31. **Novick, R. P., et al.** 1993. Synthesis of staphylococcal virulence factors is controlled by a regulatory RNA molecule. EMBO J. **12:**3967–3975.
32. **Pöhlmann-Dietze, P., et al.** 2000. Adherence of *Staphylococcus aureus* to endothelial cells: influence of capsular polysaccharide, global regulator *agr*, and bacterial growth phase. Infect. Immun. **68:**4865–4871.
33. **Sadykov, M. R., et al.** 2010. Tricarboxylic acid cycle-dependent synthesis of *Staphylococcus aureus* type 5 and 8 capsular polysaccharides. J. Bacteriol. **192:**1459–1462.
34. **Sadykov, M. R., et al.** 2008. Tricarboxylic acid cycle-dependent regulation of *Staphylococcus epidermidis* polysaccharide intercellular adhesin synthesis. J. Bacteriol. **190:**7621–7632.
35. **Sadykov, M. R., et al.** 2010. Using NMR metabolomics to investigate tricarboxylic acid cycle dependent signal transduction in *Staphylococcus epidermidis*. J. Biol. Chem. **285:**36616–36624.
36. **Sambrook, J., E. F. Fritsch, and T. Maniatis.** 1989. Molecular cloning: a laboratory manual, 2nd ed. Cold Spring Harbor Laboratory Press, Cold Spring Harbor, NY.
37. **Seidl, K., et al.** 2006. *Staphylococcus aureus* CcpA affects virulence determinant production and antibiotic resistance. Antimicrob. Agents Chemother. **50:**1183–1194.
38. **Somerville, G. A., et al.** 2002. In vitro serial passage of *Staphylococcus aureus*: changes in physiology, virulence factor production, and *agr* nucleotide sequence. J. Bacteriol. **184:**1430–1437.
39. **Somerville, G. A., et al.** 2002. *Staphylococcus aureus* aconitase inactivation unexpectedly inhibits post-exponential-phase growth and enhances stationary-phase survival. Infect. Immun. **70:**6373–6382.
40. **Somerville, G. A., et al.** 2003. Synthesis and deformylation of *Staphylococcus aureus* delta-toxin are linked to tricarboxylic acid cycle activity. J. Bacteriol. **185:**6686–6694.
41. **Somerville, G. A., and R. A. Proctor.** 2009. At the crossroads of bacterial metabolism and virulence factor synthesis in staphylococci. Microbiol. Mol. Biol. Rev. **73:**233–248.
42. **Sorensen, K. I., and B. Hove-Jensen.** 1996. Ribose catabolism of *Escherichia coli*: characterization of the *rpiB* gene encoding ribose phosphate isomerase B and of the *rpiR* gene, which is involved in regulation of *rpiB* expression. J. Bacteriol. **178:**1003–1011.
43. **Towbin, H., T. Staehelin, and J. Gordon.** 1979. Electrophoretic transfer of proteins from polyacrylamide gels to nitrocellulose sheets: procedure and some applications. Proc. Natl. Acad. Sci. U. S. A. **76:**4350–4354.
44. **Vuong, C., et al.** 2005. *Staphylococcus epidermidis* polysaccharide intercellular adhesin production significantly increases during tricarboxylic acid cycle stress. J. Bacteriol. **187:**2967–2973.
45. **Vytvytska, O., et al.** 2002. Identification of vaccine candidate antigens of *Staphylococcus aureus* by serological proteome analysis. Proteomics **2:**580–590.
46. **Yamamoto, H., M. Serizawa, J. Thompson, and J. Sekiguchi.** 2001. Regulation of the *glv* operon in *Bacillus subtilis*: YfiA (GlvR) is a positive regulator of the operon that is repressed through CcpA and *cre*. J. Bacteriol. **183:**5110–5121.
47. **Zhu, Y., et al.** 2007. *Staphylococcus aureus* biofilm metabolism and the influence of arginine on polysaccharide intercellular adhesin synthesis, biofilm formation, and pathogenesis. Infect. Immun. **75:**4219–4226.
48. **Zhu, Y., et al.** 2009. Tricarboxylic acid cycle-dependent attenuation of *Staphylococcus aureus* in vivo virulence by selective inhibition of amino acid transport. Infect. Immun. **77:**4256–4264.
49. **Zielinska, A. K., et al.** 2011. Defining the strain-dependent impact of the staphylococcal accessory regulator (*sarA*) on the alpha-toxin phenotype of *Staphylococcus aureus*. J. Bacteriol. **193:**2948–2958.